# Wearable Spirometry: Using Integrated Environment Sensor for Breath Measurement

Alejandro Baucells Costa, Bo Zhou, Orkhan Amiraslanov and Paul Lukowicz
German Research Center for Artificial Intelligence (DFKI), Kaiserslautern, Germany
Technical University of Kaiserslautern, Kaiserslautern, Germany
{Alejandro.Baucells_Costa, Bo.Zhou, Orkhan.Amiraslanov, Paul.Lukowicz}@dfki.de

***Abstract*—In this work, we present and evaluate a concept for using an integrated environment sensor as a wearable spirometer. Unlike a standard spirometer that by design is fairly bulky, our device can be unobtrusively integrated into various configurations suitable for long-term use in everyday settings (open headset, regular face mask, and professional sports mask). The sensor measures the transient change in air pressure, humidity and temperature in front of wearers' mouth and nostrils. We present our hardware design and signal analysis methods needed to extract breathing rate information. We compare the results with a standard spirometer. Moreover, a calibration between the BME280 sensor and the spirometer is performed, having both working in parallel. We show that our approach is able to distinguish between normal breaths and deep breaths, as well as to capture the period and magnitude of the breath cycles, with a wearable device that can be used in everyday scenarios, as well as sport activities. The classification accuracy is 96% in face mask settings and 82% in an open headset setting. We also show that the sensor is able to approximate air volume by comparing the sensor's pressure channel to the spirometer's flow rate results.**

***Keywords–Wearable technology; Head-mounted sensing; Spirometry; Respiration detection.***

## I. INTRODUCTION

Nowadays, wearable devices have a wide range of capabilities to monitor users' vitals and physical activities, such as heart rate and the number of steps taken; however, there has been a lack of emphasis on breathing detection during everyday scenarios.

Spirometry is an important established medical procedure to determine lung capacity and oxygen intake [1]. Studies have shown oxygen intake has a direct correlation with body composition and physical conditioning, such as cardio-respiratory performance [2][3]. Spirometry is important not only in physical fitness related activities but also in one's daily professional life.

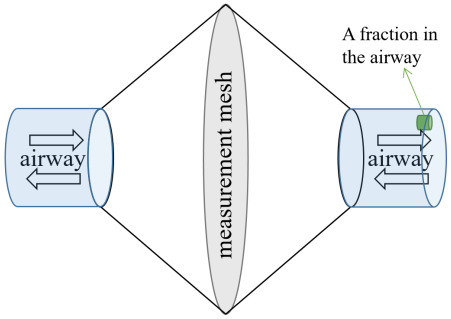


Figure 1. A common Pneumotachometer type spirometer requires all the airway directed to the sensing element.

Sigh rate is a clear indication of mental stress [4], and sufficient deep breathing can also effectively reduce stress and anxiety [5][6]. Lung capacity is also an indicator of development or stage of recovery of various illness [7][8].

However, all of the spirometry is carried out under a testing environment such as in a lab or clinic. As mentioned in various studies, such an environment cannot fully reflect every aspect of the participants' daily life [9]. The traditional digital pneumotachometer spirometer requires a fine mesh of typically 7 cm in diameter as the sensing element, as well as a mouthpiece that directs all the airflow into the sensing element, as illustrated in Figure 1. This is because the standardization of spirometry requires a laminar airflow passage that has a total resistance to the airflow at $14L \cdot s^{-1}$ smaller than $1.5cmH_2O \cdot L^{-1} \cdot s^{-1}$, considering any mechanical structure between the person and the sensing element including tubing, valves, filters, etc., as well as water vapor condensation [1]. Therefore, it is not practical to transform the traditional spirometer into a wearable device.

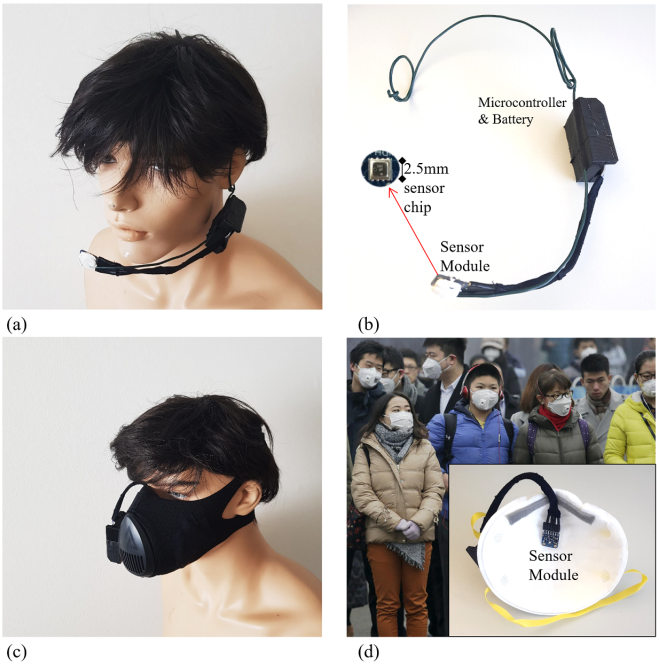


Figure 2. (a) (b) prototype as an open-air headset. (c) prototype fitted into a professional training mask (TRAINING MASK 3.0). (d) prototype fitted into a regular dust respirator (3M 8710E) [10].

The contribution of this work is three-fold:

- We have developed a wearable system to continuously monitor respiration using a small atmosphere monitoring Integrated-Circuit (IC) sensor.
- We compare our system with an off-the-shelf hand-held spirometer. The result proves there is a consistent relationship between the two different sensors during breathing.

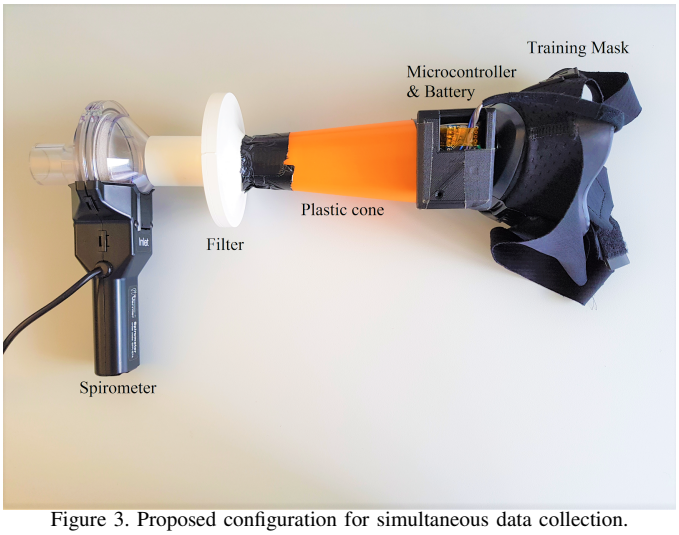

Figure 3. Proposed configuration for simultaneous data collection.

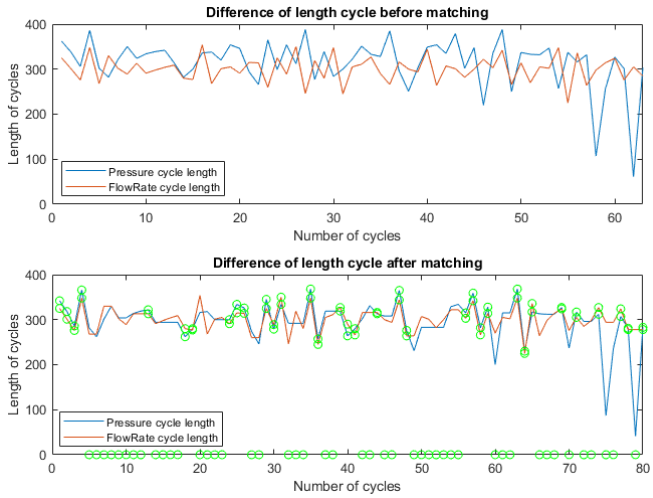

Figure 4. A difference of length cycle before vs. after thresholding

- We demonstrate that our system alone is capable of detecting breathing instances, and recognizing between normal and deep breaths.

The rest of the paper is structured as follows: In Section II, the state-of-the-art is reviewed. In Section III, the form factors of this work are described. In Section IV, the hardware and the configuration of the system are described. In Section V, we explain the first of the performed studies regarding the calibration of the system: experiments, data processing, and results. In Section VI, we expose and explain a use case study: experiments, data processing, and results. Finally, in Section VII, we conclude our work and mention new ideas to further evaluate the system.

## II. Related Work

A wide range of wearable technologies is being developed in respiratory monitoring [11]. Some examples are belt transducers that measure the change of chest perimeter such as the commercially available Pneumotrace II by AD Instruments; sternum or belly positioned smartphones recording the accelerometric signals [12]; sound based wheeze detection [13] and breathing rate detection [14]; and deriving breathing rate from pulse oximetry [15]. However, as the sensors are not directly positioned in the air flow passage, most of the modalities focus on breathing rate and not on air volume during the respiration act, and are prone to noise and motion caused influences, thus most of the studies conducted require the wearers to remain still.

## III. Form Factors

In this work, we measure the parameters of a fraction from the airflow including pressure, temperature, and humidity. These physical parameters can be measured by miniature integrated sensors, such as the Bosch BME280 with the dimension of 2.5 mm-by-2.5 mm (Figure 2(d)).

There are already several form factors where the sensors can be integrated. In many professional workplaces, there are slim headsets that position a small microphone in front of the mouth. Particularly in Asia, respiratory masks are commonly used to fend off pollen, epidemic, and pollution. While the acceptance of such surgical masks may be a matter of debate in other cultures, fashionable designs are already emerging to improve the acceptance, such as Vogmask and Airinum. In sports, there are also training masks that restricts the air intake to increase the training intensity, such as Training Mask [16] in Figure 2(c).

## IV. Prototype

We integrate the small BME280 sensor (Bosch) in each of these form factors to examine the output as the wearers do normal and deep breathing. The different settings (headset, training mask and cotton mask) are shown in Figure 2. In the headset case, the airflow out of the mouth and nostril are not directed to be focused on the sensor; for both of the masks, the sensor is in a closed chamber. The cotton mask has a filtering effect on both the inflow and outflow of air. The training mask does not have a filter, but an adjustable valve.

The system consists of a BME280 sensor measuring pressure (units in Pascal); temperature (units in Celsius) and relative humidity (units in percent) (Figure 2(d)). In our pilot study prototype, we use an Adafruit BME280 module. But the actual sensor measures only 2.5 mm, which can be easily integrated into any headpiece/mouthpiece form factors. The sensor readout is controlled by an ATMEL microcontroller through an I2C bus. The microcontroller then communicates with an RN42 module via UART, forwarding the data to an Android application for visualization and recording sensor data.

## V. System Calibration

### A. Experiment

Our goal is to investigate how the sensor data relates to an off-the-shelf spirometer in estimating the volume of air. For that reason, we are interested in capturing the actual breathed volume from both sensing systems running in parallel. In Figure 3, the proposed configuration is depicted, which consists of the spirometer and the training mask connected to each other using a plastic cone sealed on both extremes by a black tape. To evaluate this setup, 5 participants are asked to perform the following 4 experiments:

1) 3 seconds inhale, 3 seconds exhale,
2) 3 seconds inhale, 3 seconds retaining the breath, 3 seconds exhale and 3 more seconds sustaining. The whole sequence is considered a cycle,
3) monitoring breathing while watching a video,

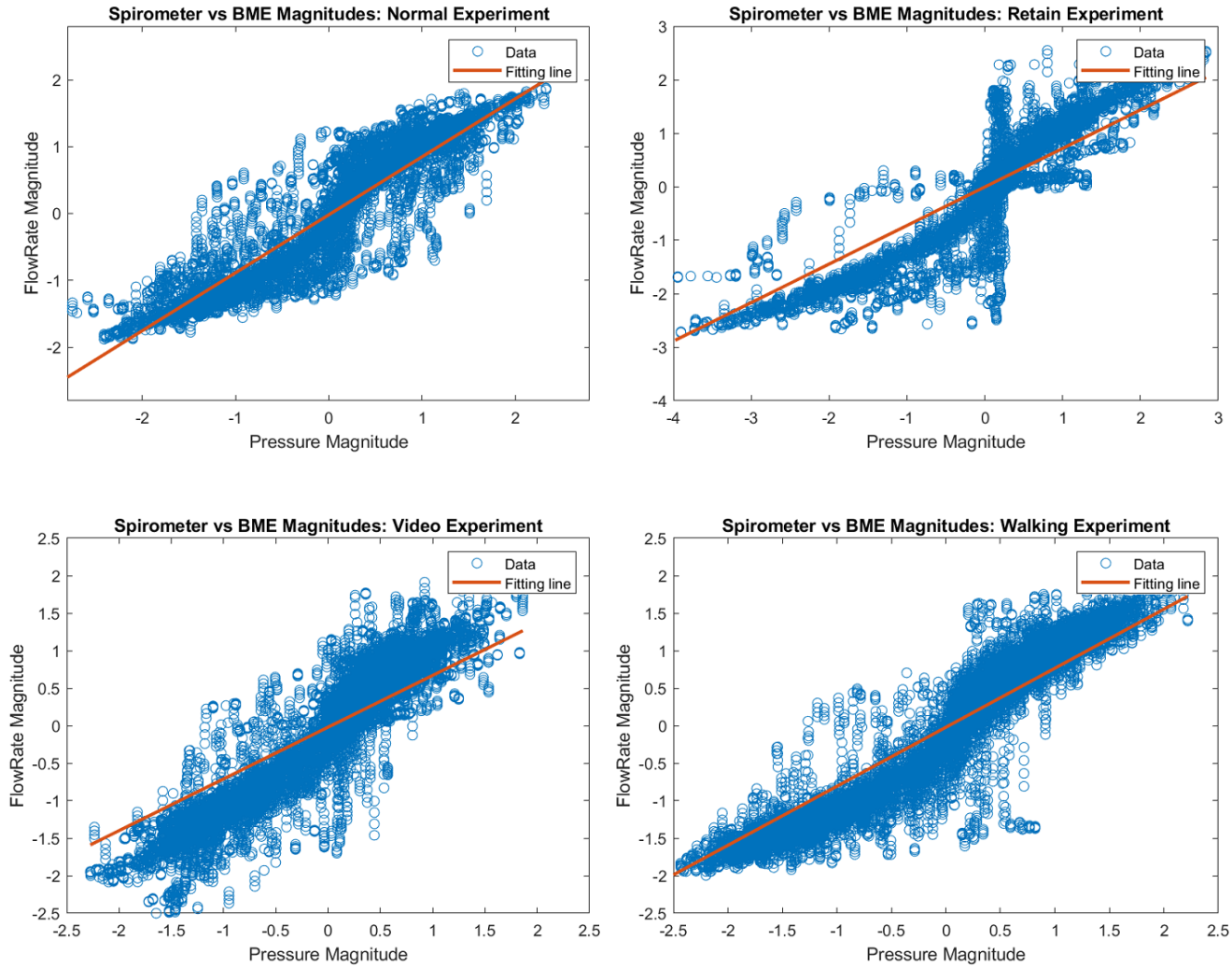


Figure 5. Magnitude relation between spirometry and BME sensor for participant 1

4) monitoring breathing while walking outdoors.

The height range of the participants is between 160 cm and 190 cm, and the weight ranges from 52.3 kg and 100 kg.

TABLE I. MAGNITUDE RELATION PARAMETERS FOR ALL PARTICIPANTS AND EXPERIMENTS

| Participant | Experiment 1 | Experiment 2 | Experiment 3 | Experiment 4 |
|---|---|---|---|---|
| 1 | std=0.328<br>slope=0.931<br>mar=0.234 | std=0.442<br>slope=0.897<br>mar=0.307 | std=0.310<br>slope=0.806<br>mar=0.222 | std=0.278<br>slope=0.951<br>mar=0.1970 |
| 2 | std=0.380<br>slope=0.896<br>mar=0.260 | std=0.553<br>slope=0.933<br>mar=0.438 | std=0.235<br>slope=0.954<br>mar=0.1503 | std=0.292<br>slope=0.923<br>mar=0.192 |
| 3 | std=0.166<br>slope=0.976<br>mar=0.128 | std=0.260<br>slope=0.937<br>mar=0.176 | std=0.174<br>slope=0.958<br>mar=0.118 | std=0.254<br>slope=0.943<br>mar=0.166 |
| 4 | std=0.6478<br>slope=0.751<br>mar=0.437 | std=0.524<br>slope=0.793<br>mar=0.432 | std=0.470<br>slope=0.772<br>mar=0.345 | std=0.390<br>slope=0.900<br>mar=0.2711 |
| 5 | std=0.531<br>slope=0.822<br>mar=0.328 | std=0.344<br>slope=1.10<br>mar=0.244 | -<br>-<br>- | std=0.245<br>slope=0.941<br>mar=0.181 |

For a more precise measure of the breathed volume, we let the users perform these 4 experiments using the mask with the sensor on it and the spirometer in parallel so that the two sensors can simultaneously capture the sequences of breathing cycles. All the experiments are recorded for 7 minutes. The Experiment 1 and 2 are performed with help of an Android application, which is intended to guide the users throughout a series of breathing routines for calming, relaxing or helping against stress. It is necessary to mention that the application has been only used to provide a visual guide to the participants, but the sequences described in there have not been followed accordingly. The third experiment is recorded while watching a video and the latest, walking outdoors. The latter two do not follow any determined cycle, only normal breath events are captured. The participants are asked to perform three fast initial exhalations as a synchronization point to facilitate the posterior analysis of the signals.

### *B. Calibration Data Processing*

Since the study involves multiple units, every experiment recording is normalized so that the average value is 0 and the standard deviation is 1.

The fact that the BME280 sensor and spirometer are placed at different locations in the airway passage may cause the signals from the two instruments to differ from each other. Especially the BME280 may be facing the nostrils and the mouth of the user in a different location and angle, because the facial structure of everyone is different. This may also contribute to deviations of the signal quality across participants.

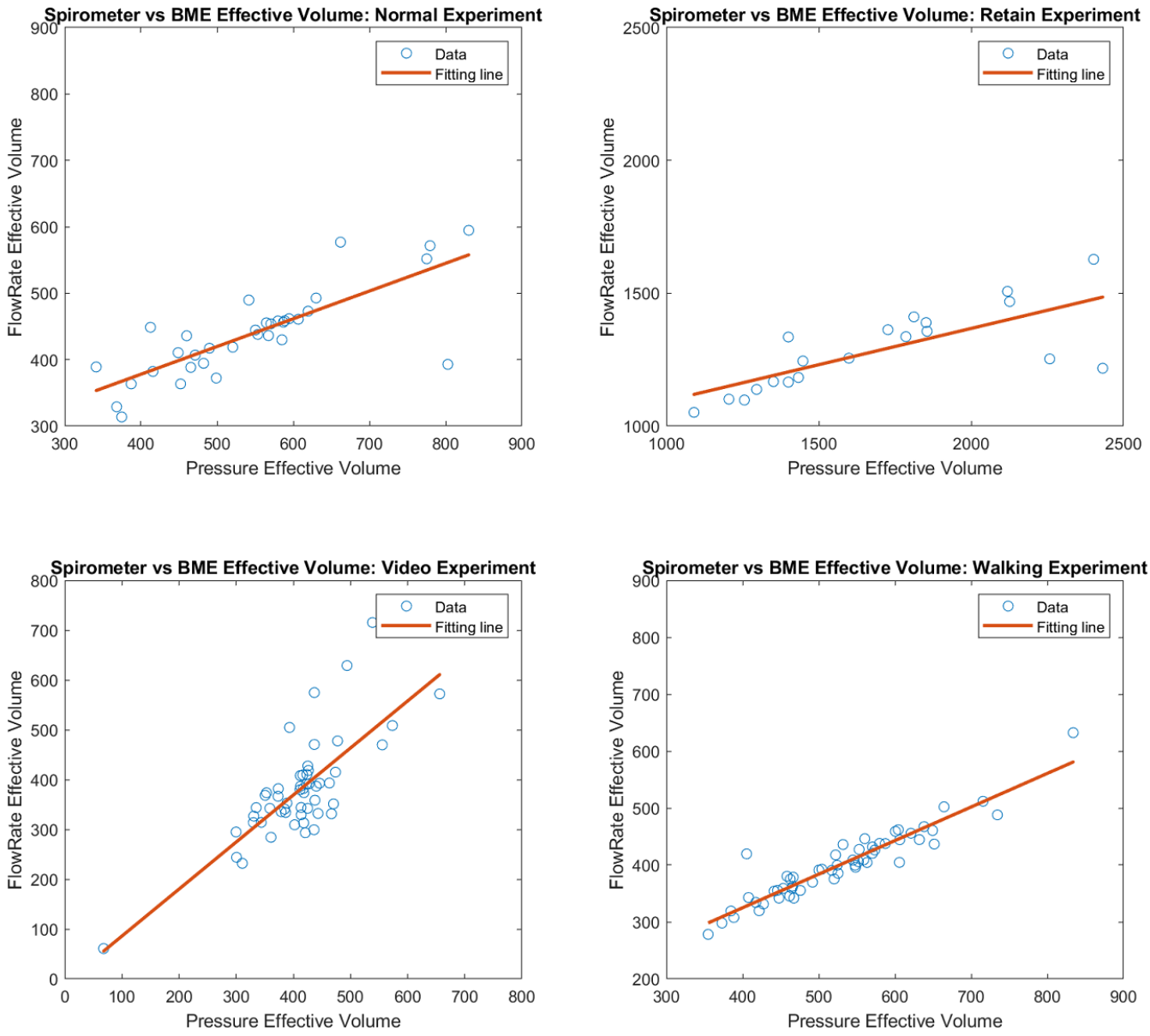


Figure 6. Effective volume relation between spirometry and BME sensor for participant 1

We chose the pressure sensor channel because it measures a similar physical parameter to the spirometer. Due to de-synchronization between the two sensors, a previous processing of the signals is necessary in order to compare the two sensors regarding matching breathing cycles. The spirometer and BME280 sensor signals are normalized and interpolated, matching their different time steps. We apply simple average filtering to remove small fluctuations in the signal samples. Then, the signals are segmented by peak detection: positive and negative peaks are located based on a prominence threshold of 20% of the signal's standard deviation. From the detected peaks, we calculate the length between each negative peak location corresponding to a breath cycle. An example is shown in Figure 4 (top). Due to interpolation, the cycles might not be perfectly aligned so a subtraction of this delay is needed, making the length of cycles from both sensors match better.

Then, we want to match the cycles that have similar length in both sensors. But there may be missing or false positive cycles in either sensor, therefore the solution is to find similar patterns in the change of cycles in both sensors. Thus *Dynamic Time Warping (DTW)* is used to match the patterns in the change of cycle lengths by finding the best matches. The result is also shown in Figure 4 (bottom). From the DTW result, it is obvious that while some cycles match exactly, some have greater differences. Except for the cases where the two cycles are actual different events, this may also be caused by the fact that from one sensor, one cycle is repeated by the DTW to 'stretch' this point so that later patterns can match the other sensor. An empirical threshold is set to eliminate those cycles whose distance is not reasonable. In Figure 4, the green marks on the plot indicate the cycles accepted by the threshold, and those at zero are rejected.

After this data processing, most of the accepted cycles are matching each other. Figure 7 illustrates 10 cycles of both

sensors cycles after processing.

### C. Results

Once subtraction for alignment and threshold for outlier elimination have been set, we extract each of those acceptable cycles to perform a deeper analysis. Those selected ones are once again interpolated and plotted. For a clearer picture of their correlation, we plot the magnitude of the pressure channel (BME280) against the magnitude of the flow rate (spirometer), resulting in Figure 5. Every point corresponds to a sensor sample. A clear positive relation is noticeable for all 4 cases. Around 0 there is a vertical belt area, where a large dispersion caused by airflow delay from the BME280 sensor's location to the spirometer, and misalignment between the two sensors, making the variance around that area larger than in the regions located on the extremes. It is especially visible in the retain experiment. Thus this vertical belt is removed in the following evaluations.

We use linear fitting within each experiment's BME280 sensor' pressure channel and spirometer's flow rate scatter plot. The vertical distance from a sensor sample point to the fitting line is the residual, which tells us how far the flow rate value of this point is away from the fitting line with the same pressure value. We use the mean value of the absolute residuals (*mar*) as a measure of how dispersed the data is away from the fitting line.

In Table I, the values for all 5 participants and the 4 experiments are depicted. Due to faulty hardware, experiment 3 for participant 5 failed.

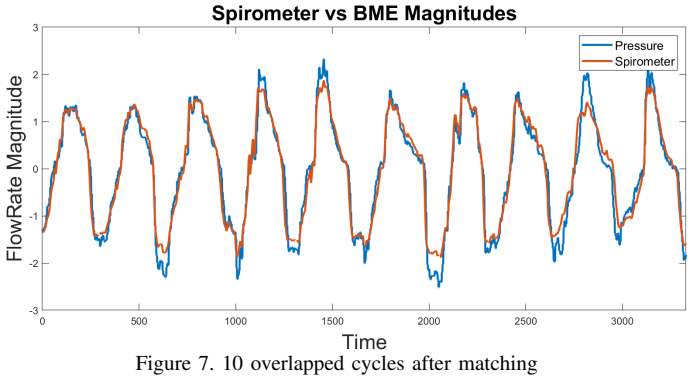

Figure 7. 10 overlapped cycles after matching

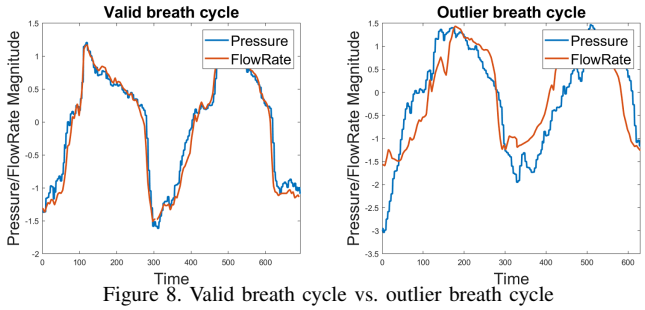

Figure 8. Valid breath cycle vs. outlier breath cycle

Even though it depends on the subject and experiment, it is possible to observe that often the *mar* values of Experiment 2 are the largest. This can be contributed to the retaining and sustaining parts of the breathing cycles described as part of Experiment 2. These assumptions could explain such values in Table I.

Later on, we calculate the 6th feature, the *Effective Volume* (explained in Section VI-B), on both training mask and spirometer data because this feature has a positive correlation with the amount of air breathed. In Figure 6, every point corresponds to a detected breathing cycle showing a linear dependency between the *Effective Volume* of pressure channel and the *Effective Volume* of the spirometer's flow rate. This means that the estimation of air volume of BME sensor and the spirometer are positively correlated. In the subplot up left of Figure 6, there are a few breathing cycles which are not close to the fitting line.

To illustrate these outlier cycles, we plot in Figure 8 one valid detected cycle against one of these such outliers so the difference between them can be observed. These outliers may not exactly be the same breathing event because the peak-to-peak distances of the two instruments do not match each other.

## VI. Use Case Study

### A. Experiment

For the headset, training mask and cotton mask cases, we invited 4, 7 and 4 people to perform experiments according to the following sequences:

1) 5 deep breaths, apnea for 5-8 seconds, and 5 more deep breaths,
2) a continuous series of 5 normal breaths, 5 deep breaths, 5 normal breaths, and 5 deep breaths,
3) a continuous series of 5 deep breaths, 5 normal breaths, and 5 deep breaths

For the training mask, the participants performed all of the 3 sequences once while seated in a room, and once walking in a hallway.

For the cotton mask and headset, only seated data is recorded. When people wear a headset, the piece pointing at the mouth may have varying distances to the mouth. Therefore, in the headset case, we let the participants adjust the piece with 2 cm, 4 cm, and 6 cm distance to the lips, and recorded the 3 sequences once in each distance.

The height range of the participants is between 160 cm and 190 cm, and the weight ranges from 52.3 kg and 100 kg. An example of the resultant signals from the second sequence in each of the cases can be observed in Figure 9. We use a spirometer SPR-BTA Inlet Vernier for reference, letting the 7 participants from the training mask perform the same sequences with the spirometer while seated. The spirometer airflow signal of the same participant from Figure 9 is shown in Figure 10.

From Figure 9, it is obvious that pressure, temperature, and humidity behave differently in the three settings. In the open-air headset setting, the air pressure is greatly influenced by the environment and only gives visible peak under a deep breath. Temperature and humidity offer a distinguishable signal, but have a drifting effect: both values increase with continuous deep breath and decrease with a normal breathing. The average values of all three channels are also lower than the other two settings which are in a closed chamber.

In the cotton mask setting, the humidity is always saturated to 100% due to the filtering material blocks humidity from dissipating. Pressure and temperature show clear distinguishable signals for normal and deep breathing. The temperature still

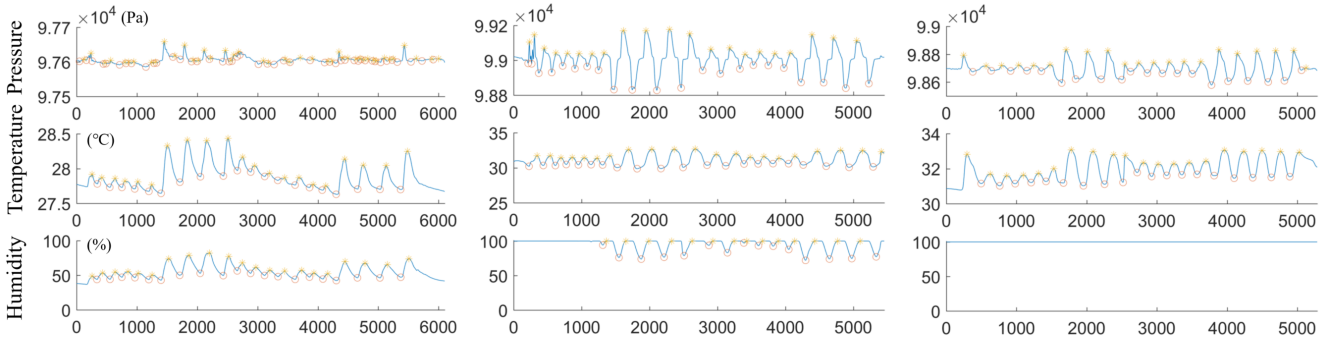


Figure 9. Signal examples from the BME280 sensor in different form factors of the participant performing alternating sequences of normal and deep breaths, the sampling rate is 50Hz

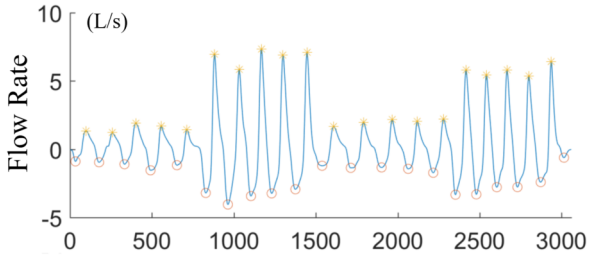


Figure 10. Signal example from the spirometer of the participant performing alternating sequences of normal and deep breaths, the sampling rate is 50Hz

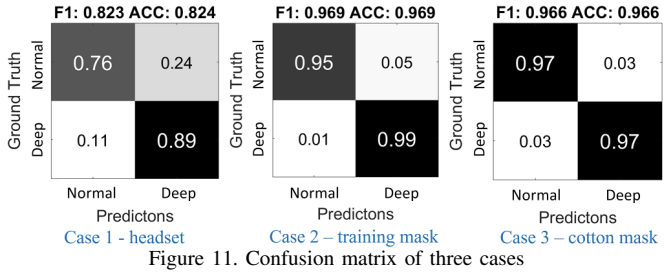


Figure 11. Confusion matrix of three cases

shows slight drifting, which is possibly contributed by the heat isolation property of the material.

In the training mask setting, the pressure and temperature showed a similar response with the cotton mask. The difference of the training mask is that the air flow in and out of the mask is an open, unfiltered airway. This contributes to less shifting in the temperature value, and the humidity is also no longer always saturated.

### B. Machine Learning Data Processing

First, the same normalization method is applied to the signal for every experiment recording in its entirety. We apply simple average filtering with a kernel size of 1-by-15 to remove small fluctuations in the signal sample. The signal is then segmented by peak detection: positive and negative peaks are located based on a prominence threshold of 20% of the signal's standard deviation, as shown in Figure 9. Since the experiment only included normal breathing paces, if there are multiple negative peaks within 2 seconds, only the deepest peak is kept. A negative peak between two positive peaks is marked as a segment point, the signal between two of these points is taken as one breathing instance or one window. Every instance is manually annotated as ground truth by assigning normal and deep breath labels. The precision and recall of detecting a breath through said peak detection are 95.6% and 99.1%.

For every breathing instance $D(t)$, we calculate the following features to represent the signal:

1) average value of $D(t)$,
2) absolute range: $max(D(t)) - min(D(t))$,
3) standard deviation of $D(t)$,
4) kurtosis of $D(t)$,
5) length of the window (negative peak-to-peak distance),
6) effective volume: first $Base(D(t))$ is calculated as the linear function that connects $D(first)$ and $D(last)$, then the sum value of $D(t) - Base(D(t))$ is taken as the effective volume.

### C. Recognizing Breath Types

From visual inspection of the data, we selected the optimal sensor channel for every case: headset - temperature, training mask - pressure, cotton mask - pressure. Although other channels may also be possible for a candidate, such as the humidity in the headset case and the temperature in both mask cases, how to combine different sensor channels will be part of the future work.

For each participant, we evaluate how well the normal and deep breaths can be separated by cross-validation using a cubic Support Vector Machine (SVM) classifier with the six features. Figure 11 shows the result as confusion matrices. The value in every cell is the summary of the individual results and normalized to the total amount of ground truth samples. The accuracy is above 96% in training mask and cotton mask cases, while 82.4% in the open-air headset case. This also agrees with the signal examples in Figure 9 and suggests that the sensors perform better in a restricted airflow for detecting normal and deep breaths.

Next, we use the Neighborhood Component Analysis (NCA) [17] to decide which features play more important roles in separating the two different breathing types. NCA takes the prediction accuracy as a goal function of additionally assigned weights to the features for every observation as variables. The goal function is continuously differentiable, thus the local maxima point can be found with optimization algorithms, where a combination of the feature weights results in a maximum prediction accuracy.

We use the `fscnca` method implemented in the Matlab Machine Learning Toolbox with default settings to perform

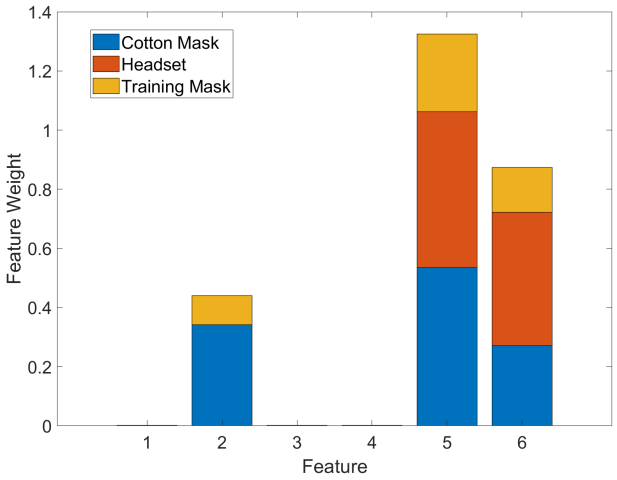

Figure 12. Feature weight after neighborhood component analysis.

NCA on a per-person basis, and then calculate the average weight for each feature within every form factor. The resulting featherweights are shown in Figure. 12. A higher value means the corresponding feature is more relevant for recognition. From the result, the 5th feature (window length) and the 6th feature (effective volume) are more relevant in all three form factors. For the cotton mask and training mask form factors, the 2nd feature (absolute range) is also relevant. The remaining features have close to zero weight. This result can be used to further optimize the feature calculation process.

## VII. Conclusion and Future Work

From our pilot study, it is clear that the integrated atmosphere sensor, which measures air pressure, temperature and humidity, can be used to detect breathing events and distinguish normal and deep breaths in different form factors including face masks and an open-air headset, thanks to the small footprint of the sensor. The algorithm consists of simple filtering, peak detection, and 6 features are calculated. The sensor is also shown to be able to estimate the air volume by comparing with a spirometer.

In our future work, we will work on improving the accuracy of detecting deep and normal breaths for the reasons that this form factor is more acceptable and can be integrated with other head-mounted wearable devices, such as headphones or smart glasses. In particular, we will investigate utilizing more than one channel instead of selecting a single optimal channel, or using two opposite-facing sensors as a differential setting to reduce the influence of the environment.

We will also conduct experiments in outdoor or more active scenarios, and use case studies especially in sport and fitness, including user feedback and assisted training.

## References

[1] M. Miller and J. Hankinson, "Standardisation of spirometry," European respiratory journal, vol. 26, no. 2, 2005, pp. 319–338.

[2] E. Buskirk and H. Taylor, "Maximal oxygen intake and its relation to body composition, with special reference to chronic physical activity and obesity," Journal of applied physiology, vol. 11, no. 1, 1957, pp. 72–78.

[3] H. Taylor, E. Buskirk, and A. Henschel, "Maximal oxygen intake as an objective measure of cardio-respiratory performance," Journal of applied physiology, vol. 8, no. 1, 1955, pp. 73–80.

[4] E. Vlemincx, J. Taelman, S. De Peuter, I. Van Diest, and O. Van Den Bergh, "Sigh rate and respiratory variability during mental load and sustained attention," Psychophysiology, vol. 48, no. 1, 2011, pp. 117–120.

[5] E. Vlemincx, J. Taelman, I. Van Diest, and O. Van den Bergh, "Take a deep breath: the relief effect of spontaneous and instructed sighs," Physiology & Behavior, vol. 101, no. 1, 2010, pp. 67–73.

[6] R. Brown and P. Gerbarg, "Sudarshan kriya yogic breathing in the treatment of stress, anxiety, and depression," Journal of Alternative & Complementary Medicine, vol. 11, no. 4, 2005, pp. 711–717.

[7] T. Kavanagh et al., "Peak oxygen intake and cardiac mortality in women referred for cardiac rehabilitation," Journal of the American College of Cardiology, vol. 42, no. 12, 2003, pp. 2139–2143.

[8] J. Stocks and P. H. Quanjer, "Reference values for residual volume, functional residual capacity and total lung capacity," European Respiratory Journal, vol. 8, no. 3, 1995, pp. 492–506.

[9] F. Swart, M. M. Schuurmans, J. C. Heydenreich, C. H. Pieper, and C. T. Bolliger, "Comparison of a new desktop spirometer (spirospec) with a laboratory spirometer in a respiratory out-patient clinic," Respiratory care, vol. 48, no. 6, 2003, pp. 591–595.

[10] "Chinadaily." [Online]. Available: https://www.ChinaDaily.com.cn [retrieved October 2018]

[11] A. Aliverti, "Wearable technology: role in respiratory health and disease," Breathe, vol. 13, no. 2, 2017, p. e27.

[12] F. Landreani and A. Martin-Yebra, "Respiratory frequency estimation from accelerometric signals acquired by mobile phone in a controlled breathing protocol," in Computing in Cardiology, 2018, pp. 1–4.

[13] S. Li, B. Lin, C. Tsai, C. Yang, and B. Lin, "Design of wearable breathing sound monitoring system for real-time wheeze detection," Sensors, vol. 17, no. 1, 2017, p. 171.

[14] A. Martin and J. Voix, "In-ear audio wearable: Measurement of heart and breathing rates for health and safety monitoring," IEEE Transactions on Biomedical Engineering, vol. 65, no. 6, 2018, pp. 1256–1263.

[15] A. Fusco, D. Locatelli, F. Onorati, G. Durelli, and M. Santambrogio, "On how to extract breathing rate from ppg signal using wearable devices," in Biomedical Circuits and Systems Conference (BioCAS), 2015 IEEE. IEEE, 2015, pp. 1–4.

[16] "Training mask l.l.c." [Online]. Available: https://www.trainingmask.com [retrieved October 2018]

[17] W. Yang, K. Wang, and W. Zuo, "Neighborhood component feature selection for high-dimensional data." JCP, vol. 7, no. 1, 2012, pp. 161–168.